Volume 354, Nos. 52–54, 15 December 2008

ISSN 0022-3093

ELSEVIER

JOURNAL OF
NON-CRYSTALLINE SOLIDS

Editor: **J.H. Simmons,** *Tucson, AZ, USA*
Co-editor: **B.G. Potter,** *Tucson, AZ, USA*

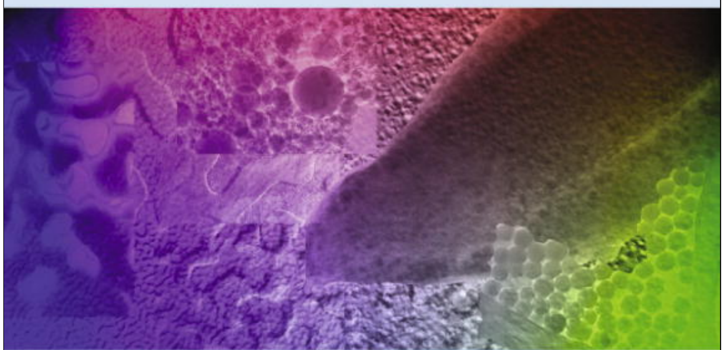

Journal of Non-Crystalline Solids 354 (2008) 5440–5443

Contents lists available at ScienceDirect

Journal of Non-Crystalline Solids

journal homepage: www.elsevier.com/locate/jnoncrysol

Minor addition induced enhancement of strength of Mg-based bulk metallic glass

J.Q. Wang, P. Yu, H.Y. Bai *

Institute of Physics, Chinese Academy of Sciences, The 3rd South Street, No. 8, Zhong, Beijing 100080, PR China

ARTICLE INFO

Article history:
Received 13 June 2008
Received in revised form 17 August 2008
Available online 7 October 2008

PACS:
61.43.Dq
81.05.Kf
62.20.Dc

Keywords:
Amorphous metals
Metallic glasses

ABSTRACT

We report that the fracture strength of Mg-based bulk metallic glasses (BMGs) can be dramatically enhanced up to 1.10 GPa by minor Gd addition. The Poisson's ratio v of the BMG also decreases to 0.261 close to that of brittle oxide glasses when 1 at.% Gd was added. Such significant enhancement in strength which approaches the theoretical strength value and dramatically decrease in the Poisson's ratio are attributed to the structural change of the BMGs induced by the Gd minor addition.

1. Introduction

High strength is one of the most important properties for engineering materials. The theoretical strength of a material is estimated to be in the order of $E/5$ (E is Young's modulus) for fracture strength or $\sim 0.1\ G$ (G is shear modulus) for shear strength based on the Frenkel model [1]. While the defects and the fabrication flaws cause the fracture of a material to occur at applied press that much lower than the theoretical value. In metallic glasses, their strength is expected to be close to the theoretical value, while the experimental facts show that the highest strength of the metallic glasses is also about 3–4 times smaller than the theoretical strength [2]. Extensive efforts have been made to strengthen the structural materials (such as nanocrystallization of a material [3], introducing poly-phases [4], and reducing the sample size [5]) and to understand the underlying mechanism for strength of materials.

Rare-earth (RE) elements are good candidates both for the fabrication of bulk metallic glasses (BMGs) as the base elements and as the microalloying elements [6–8]. The glass forming ability [7,9], mechanical and physical properties [7–8] can be greatly improved or changed by the RE minor addition. Mg-based BMG is a promising candidate for engineering materials such as automobile, aircraft industries because of its marvelous mechanical properties such as light density, high specific strength, and low-cost. However, the Mg-based BMGs have relatively low strength compared to that of other known BMGs, and their fracture strength is found to be 600–850 MPa depending on the composition [10–12].

In this work, we report that the mechanical properties of the Mg-based BMGs can be much improved by minor Gd addition. The fracture strength of the Mg-based BMGs is much enhanced accompanying with the obvious Poisson's ratio change when minor Gd is added. The structural inhomogeneity in micrometer scale is attributed to the enhancement of the fracture strength of the Mg-based BMGs. The results are suggestive for improvement of the mechanical properties of metallic glasses.

2. Experimental

The pure Cu, Y, and Gd (purity better than 99.9 at.%) elements were arc melt under a Ti-gettered Ar atmosphere to get the ingot. The CuYGd ingot was then induction melt together with Mg (purity 99.99 at.%) with nomination composition of $Mg_{65}Cu_{25}Y_{10-x}Gd_x$ ($x = 1, 2, 5, 8$) in a quartz tube under vacuum (better than 3.0×10^{-3} Pa). The MgCuYGd melt was then cast into a Cu mold to get amorphous rods or plates. The details for the bulk metallic glasses formation can be referred as to Refs. [2,13]. The amorphous nature of the as-cast samples was confirmed by X-ray diffraction (XRD) in a MAC M03 XHF diffractometer by using Cu K_α radiation. The thermal analysis of the alloys were performed by the differential scanning calorimeter (DSC) using a Perkin–Elmer DSC-7 under flowing purified argon with a heating rate of 20 K/min. The thermodynamic parameters such as glass transition temperature T_g,

* Corresponding author.
E-mail address: hybai@aphy.iphy.ac.cn (H.Y. Bai).

0022-3093/$ - see front matter © 2008 Elsevier B.V. All rights reserved.
doi:10.1016/j.jnoncrysol.2008.08.010

crystallization temperature of T_x, and melting temperature T_m were determined with an accuracy of ±1 K. The glassy structure of the alloy was confirmed by high-resolution transmission electron microscopy (HRTEM) and selected area electron diffraction (SAED) on a Philips CM200EG machine operated at 200 kV. The acoustic velocities were measured using a pulse echo overlap method by a MATEC 6600 model ultrasonic system with a measuring sensitivity of 0.5 ns and carry frequency of 10 MHz [2]. The density was determined by the Archimedean principle and the accuracy is about 0.5%. The Young's modulus E, shear modulus G, bulk modulus K and Poisson's ratio v were derived from the density and acoustic velocities with an accuracy of 1% [2]. The samples with a gauge aspect ratio of 2:1 were cut out of the as-cast 2-mm rods for uniaxial compression tests on an Instron 5500R1186 machine. The average yield strength was determined by the for uniaxial compression tests, and for each alloy the number of compression tests is 5. The accuracy for the strength measurements is about 5%.

3. Results

Fig. 1 shows the XRD patterns, DSC traces, HRTEM and SAED images of the $Mg_{65}Cu_{25}Y_{10-x}Gd_x$ BMGs. The XRD patterns show broad diffraction maxima characteristic of glass without obvious crystalline Bragg peaks (Fig. 1(a)). The DSC traces (see inset of Fig. 1(a)) show distinct glass transition temperature T_g, sharp crystallization exothermic peak and large supercooled liquid region. The HRTEM image (Fig. 1b) shows a mazelike pattern without any crystalline feature and the SAED pattern (Inset of Fig. 1(b)) shows the faint and diffuse ring. All these results confirm the alloy consists of full glassy state without crystalline phases within the detecting limit of these instruments.

The compression curve of the $Mg_{65}Cu_{25}Y_9Gd_1$ BMG is shown in the inset of Fig. 2. The stress versus strain shows a linear behavior up to about 2.2%, indicating the large elastic limit of 2.2%. The glassy alloy fails immediately without obvious plasticity, and the fracture strength is about 1.06 GPa. The remarkable features of the additional BMG samples are high strength and large elasticity (2.2%). The fracture strength σ_f of $Mg_{65}Cu_{25}Y_{10}$ BMGs is only ~0.68 GPa, and for ternary $Mg_{65}Cu_{25}Gd_{10}$ σ_f is 0.83 GPa [12,14]. Remarkably, the σ_f of the $Mg_{65}Cu_{25}Y_9Gd_1$ increases sharply to ~1.0 GPa with only 1 at.% Gd addition. The σ_f values keep larger than 1 GPa for 1–8 at.% Gd addition. The maximum σ_f of 1.11 GPa, which is 66% larger than that of the ternary $Mg_{65}Cu_{25}Y_{10}$ BMG, is obtained with 5 at.% Gd addition. A linear correlation between yielding shear stress τ_Y (=σ_f/2) and shear modulus G has been reported with $\tau_Y/G \sim 0.0267$ [15]. For the $Mg_{65}Cu_{25}Y_{10-x}Gd_x$ BMGs with $x = 0$, 1, 2, 5, 10, the value of τ_Y/G is determined to be 0.0180, 0.0272, 0.0257, 0.0282, and 0.0216, respectively. As shown in Fig. 2(b), the values for the Gd-additional quaternary alloys are much larger than that of the $Mg_{65}Cu_{25}Y_{10}$ BMG, and the strength of the Gd-additional BMGs is closer to their theoretical shear stress value.

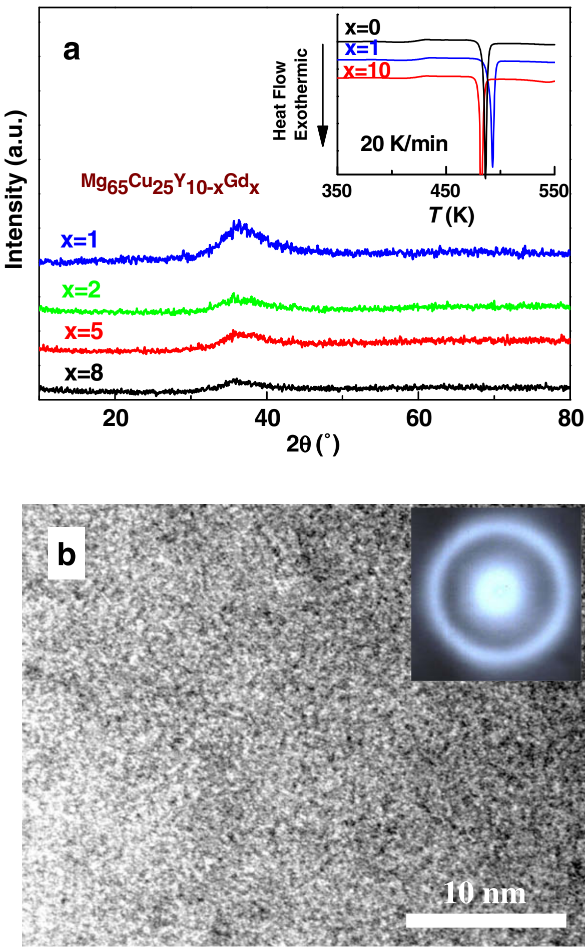

Fig. 1. (a) XRD curves of the $Mg_{65}Cu_{25}Y_{10-x}Gd_x$ ($x = 1, 2, 5, 8$) BMGs. Inset: The DSC traces of $x = 0$, 1, 10 samples. (b) The HRTEM image and SAED pattern of $x = 1$ sample (with a heating rate of 20 K/min).

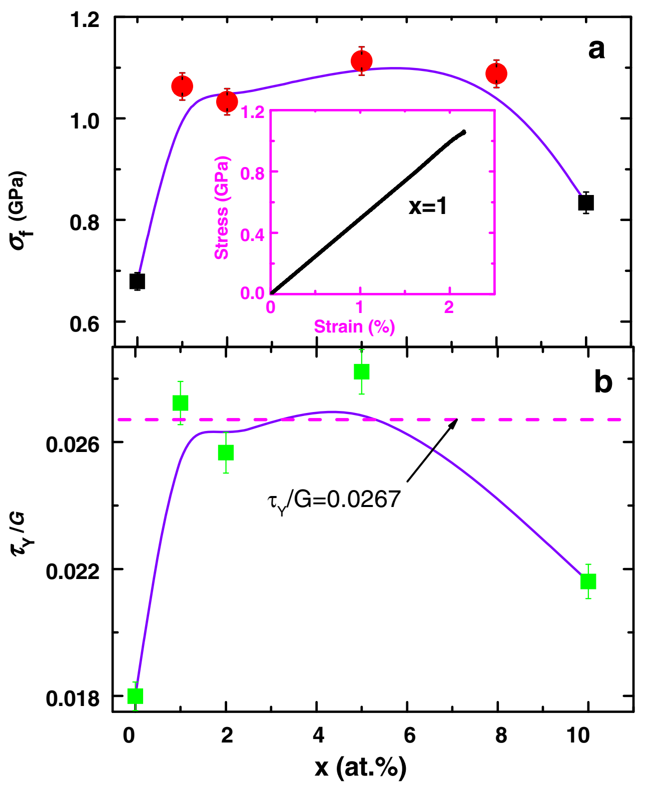

Fig. 2. (a) Fracture stress σ_f of $Mg_{65}Cu_{25}Y_{10-x}Gd_x$ system versus the concentration of Gd. The maximum σ_f is 1.11 GPa for $Mg_{65}Cu_{25}Y_5Gd_5$, which is about 1.66 times of $Mg_{65}Cu_{25}Y_{10}$ and 1.33 of $Mg_{65}Cu_{25}Gd_{10}$. The blue line is for guiding the eyes. Inset: The uniaxial compression curve of $Mg_{65}Cu_{25}Y_9Gd_1$. (b) The ratio of τ_Y/G was enhanced greatly by Gd-microalloying. The blue line is for guiding the eyes. The magenta dash-dot line shows the τ_Y/G value of 0.0267 for various BMGs Ref. [15]. (For interpretation of the references in colour in this figure legend, the reader is referred to the web version of this article.)

For most BMGs such Zr- and Cu-based BMGs, abundant observations show that these BMGs always fracture along a plane deviating from the maximum shear stress plane [2]. The metallic glassy specimens normally preferentially fracture along the maximum shear stress plane and the compressive axis and the fracture plane is about 45°. SEM was performed on the fracture samples of our Mg-based BMG as shown in Fig. 3(a). Few shear bands are observed near the fracture surface, which confirms the high strength and brittle nature of the BMGs. Under uniaxial compression, for conventional BMGs, the specimens normally preferentially fracture along the maximum shear stress plane and the compressive axis and the inner strength direction is about 45°, and fracture into two parts. While the additional Mg-based BMG samples fractured not in a shear behavior occurring in conventional BMGs but in an exploding way and crack into many small pieces as shown in Fig. 3(c). Meanwhile, the fracture surface shows a complex landscape (Fig. 3(b)) suggesting that the vicinity of the surface has been bearing rather intricate tensile strength when compressing. The small fractured pieces support the image of intricate tensile strength [16–17].

The toughness of BMGs is reported to correlate with Poisson's ratio ν [18,19]. The smaller the ν is, the more brittle the BMGs become. This correlation was verified in various BMGs with markedly different plasticity [20–22]. The mass densities ρ and the elastic moduli at room temperature for $Mg_{65}Cu_{25}Y_{10-x}Gd_x$ system are shown in Table 1. The density of the samples increase monotonously with the addition of Gd indicating the dense of glass with Gd addition. The Gd addition induces denser atomic-scale packing due to the arrangement of atomic species during solidification. Comparing with the ternary $Mg_{65}Cu_{25}Y_{10}$ and $Mg_{65}Cu_{25}Gd_{10}$ BMGs [13], the $Mg_{65}Cu_{25}Y_{10-x}Gd_x$ BMGs possess smaller bulk modulus and ν. The $Mg_{65}Cu_{25}Y_9Gd_1$ BMG has the lowest value of Poisson's ratio of 0.261 among the known BMGs as shown in Fig. 4. The small ν is consistent with the extreme brittle nature of the BMGs. According to the correlation between the Poisson's ratio and toughness of the BMGs, the BMG should have very low fracture toughness [18,19].

Table 1
The density ρ, the shear modulus G, Young's modulus E, bulk modulus K, Poisson's ratio ν, and fracture strength σ_f for $Mg_{65}Cu_{25}Y_{10-x}Gd_x$ (x = 0, 1, 2, 5, 10)

	ρ (g/cm^3) (±0.5%)	G (GPa) (±1%)	E (GPa) (±1%)	K (GPa) (±1%)	ν (±1%)	σ_f (GPa) (±5%)
$Mg_{65}Cu_{25}Y_{10}$	3.284	18.9	50.1	48.8	0.329	0.68
$Mg_{65}Cu_{25}Y_9Gd_1$	3.336	19.5	49.2	34.3	0.261	1.06
$Mg_{65}Cu_{25}Y_8Gd_2$	3.429	20.1	51.7	39.9	0.284	1.03
$Mg_{65}Cu_{25}Y_5Gd_5$	3.650	19.7	50.6	39.1	0.284	1.11
$Mg_{65}Cu_{25}Gd_{10}$	3.79	19.3	50.6	45.1	0.313	0.83

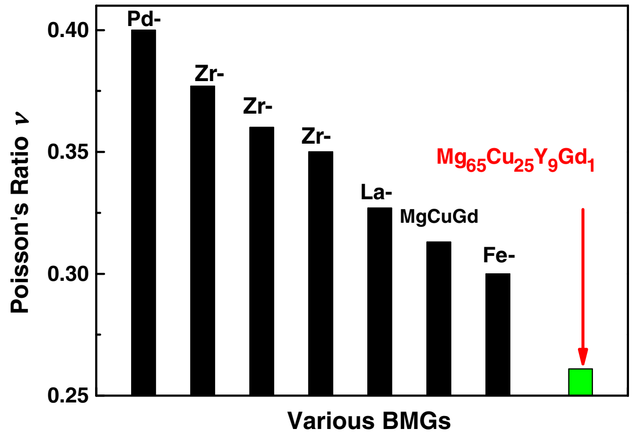

Fig. 4. The comparison of Poisson's ratio of several typical BMGs (Pd-based BMG Ref. [1,8], Zr-based BMGs Ref. [2], La-based BMG Ref. [2], MgCuY BMG Ref. [2], Fe-based BMG [2,8]). The $Mg_{65}Cu_{25}Y_9Gd_1$ has the lowest value of 0.261.

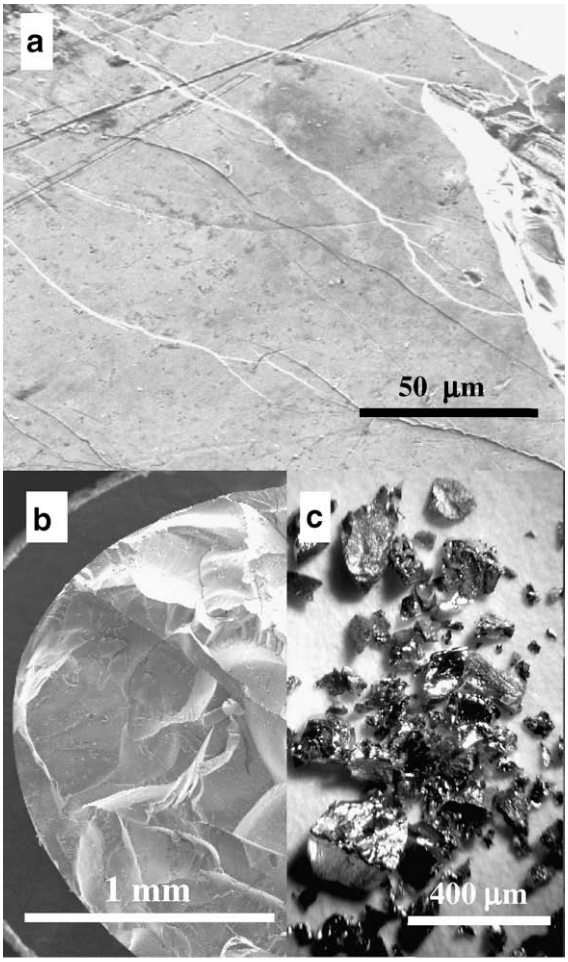

Fig. 3. (a) Few shear bands were observed only near the fracture surface. (b) The complex landscape of the fracture surface after uniaxial compression. (c) The samples break into the small pieces in an exploding way.

4. Discussions

The effects of Gd microalloying on the fracture strength could be understood in microstructural point of view: the addition of minor Gd can densify the BMG by remove the free volumes due to denser atomic-scale packing and the rearrangement of atomic species during solidification, which is verified by the density measurements. The density is increased with more Gd addition even we rule out the density increase induced by Gd density itself. Actually, the minor additions are widely applied to reduce the fraction of the defects in materials and strengthen the material for approaching the theoretical strength value [5,23]. The dense microstructure with fewer fractions of free volumes and flaws often induce low value of the Poisson's ratio which is agreement with our experimental results [8]. The low ν confirms that the sample has good ability to resist from shearing deformation and failure under uniaxial compression. This is consistent with the observed results of few shear bands (Fig. 3(a)) and high fracture strength (Fig. 2) of the BMG.

The Gd-additional could dramatically change the microstructure of the BMGs which induce enhanced strength. A recent study has revealed that the minor Co addition dramatic increase the cluster (the building block of the BMGs [24]) symmetry in CeCuAl BMG of Al site, which, in turn, increase the glass forming ability of the alloy greatly [25–26]. The results may shed light on understanding our results. Gd minor addition might change the local symmetry of clusters in the Mg-based BMG and the high symmetry building blocks (or clusters) could be the main reason for the dense microstructure of the BMGs which derive in the change of mechanical properties.

5. Conclusions

We report that the fracture strength of Mg-based BMGs can be significantly enhanced up to 1.1 GPa using Gd minor addition. Such a enhancement in strength is attributed to structural change of the BMG induced by Gd addition. The results indicate that the addition method may be a good way to increase the shear yielding stress without obvious change of shear modulus. The results may be suggestive for improvement of the mechanical properties of metallic glasses.

Acknowledgements

The discussions with Professor W.H. Wang, R.J. Wang, D.Q. Zhao, M.X. Pan are appreciated. The financial support of the NSF of China (Grant Nos. 50671117, 50621061 and 50731008) and MOST 973 (2007CB613904) are appreciated.

References

[1] G.E. Dieter, Mechanical Metallurgy, McGraw-Hill, New York, 1986. p. 119.
[2] W.H. Wang, C. Dong, C.H. Shek, Mater. Sci. Eng. R 44 (2004) 45.
[3] Y.M. Wang, M.W. Chen, F.H. Zhou, E. Ma, Nature 419 (2002) 912.
[4] C.C. Hays, C.P. Kim, W.L. Johnson, Phys. Rev. Lett. 84 (2000) 2901.
[5] Z.W. Shan, R.K. Mishra, S.A. Syed Asif, O.L. Warren, A.M. Minor, Nat. Mater. 7 (2008) 115.
[6] B. Zhang, D.Q. Zhao, M.X. Pan, W.H. Wang, A.L. Greer, Phys. Rev. Lett. 94 (2005) 205502.
[7] (a) P. Yu, H.Y. Bai, W.H. Wang, J. Mater. Res. 21 (2006) 1674;
(b) M.B. Tang, D.Q. Zhao, M.X. Pan, W.H. Wang, China Phys. Lett. 21 (2004) 901;
(c) W.H. Wang, J.J. Lewandowski, A.L. Greer, J. Mater. Res. 20 (2005) 2307;
(d) W.H. Wang, Z.X. Bao, J. Eckert, Phys. Rev. B 61 (2000) 3166.
[8] (a) W.H. Wang, Prog. Mater. Sci. 52 (2007) 540;
(b) W.H. Wang, Z. Bian, P. Wen, Y. Zhang, M.X. Pan, D.Q. Zhao, Intermetallics 10 (2002) 1249.
[9] H.J. Wang, G.J. Shiflet, S.J. Poon, K. Matsuda, S. Ikeno, Appl. Phys. Lett. 91 (2007).
[10] D.G. Pan, H.F. Zhang, A.M. Wang, Z.Q. Hu, Appl. Phys. Lett. 89 (2006) 261904.
[11] Q. Zheng, S. Cheng, J.H. Strader, E. Ma, J. Xu, Scripta Mater. 56 (2007) 161.
[12] G.Y. Yuan, A. Inoue, J. Alloys Compd. 387 (2005) 134.
[13] X.K. Xi, R.J. Wang, D.Q. Zhao, M.X. Pan, W.H. Wang, J. Non-Cryst. Solids 344 (2004) 105.
[14] (a) K. Amiya, A. Inoue, Mater. Trans., JIM 41 (2000) 1460;
(b) Y. Zhang, D.Q. Zhao, W.H. Wang, J. Non-Cryst. Solids 315 (2003) 206.
[15] W.L. Johnson, K. Samwer, Phys. Rev. Lett. 95 (2005) 195501.
[16] X.K. Xi, D.Q. Zhao, M.X. Pan, W.H. Wang, Y. Wu, J.J. Lewandowski, Phys. Rev. Lett. 94 (2005) 125510.
[17] G. Wang, D.Q. Zhao, H.Y. Bai, M.X. Pan, X.K. Xi, Y. Wu, W.H. Wang, Phys. Rev. Lett. 98 (2007) 235501.
[18] W.H. Wang, J. Appl. Phys. 99 (2006) 093506.
[19] J.J. Lewandowski, W.H. Wang, A.L. Greer, Philos. Mag. Lett. 85 (2005) 77.
[20] X.J. Gu, S.J. Poon, A.G. McDermott, G.J. Shiflet, Appl. Phys. Lett. 88 (2006) 211905.
[21] Y.H. Liu, G. Wang, D.Q. Zhao, W.H. Wang, Science 315 (2007) 1385.
[22] P. Yu, R.J. Wang, H.Y. Bai, Mater. Sci. Eng. A 485 (2008) 1.
[23] H. Bei, Z.P. Lu, E.P. George, Phys. Rev. Lett. 93 (2004) 125504.
[24] D. Miracle, Nat. Mater. 3 (2004) 697.
[25] X.K. Xi, L.L. Li, B. Zhang, W.H. Wang, Y. Wu, Phys. Rev. Lett. 99 (2007) 095501.
[26] B.A. Sun, M.X. Pan, W.H. Wang, X.K. Xi, Y. Wu, Scripta Mater. 59 (2008) 1159.